01,05,08,18

Anisotropy of the Paramagnetic Susceptibility in the 3D Dirac Semimetal Cd_3As_2 Caused by Chromium Impurity: the EPR on Cr^{3+} Ions

© Yu.V. Goryunov[1], A.N. Nateprov[2]

[1] FRC Kazan Scientific Center RAS,
Kazan, Russia
[2] Institute of Applied Physics, Moldova State University,
Chişinău MD2028, Republic of Moldova

E-mail: gorjunov@kfti.knc.ru

Received December 15, 2022
Revised December 15, 2022
Accepted December 22, 2022

In the literature devoted to magnetic impurities in Dirac semimetals, the appearance of anisotropic and long-range non-oscillating contributions to the Ruderman–Kittel–Kasuya–Yosida interaction is predicted. These contributions are due to the hybridization of the wave functions of magnetic impurities with the wave functions of Dirac electrons, which have a linear dispersion law. We have studied electron paramagnetic resonance (EPR) in powder samples of topological 3D Dirac semimetal Cd_3As_2 with an admixture of chromium ions. Anisotropy of the magnetic susceptibility in the paramagnetic state was found from the behavior of the resonance field. The appearance of magnetic anisotropy in the paramagnetic state is associated with an increase in the contribution of the orbital moments of chromium ions Cr^{2+} and Cr^{3+} due to their interaction with the orbital moments of donor Dirac electrons, which have anomalously large values of g factors.

Keywords: magnetic resonance, topological materials, magnetic impurities.

DOI: 10.21883/PSS.2023.03.55575.553

1. Introduction

A characteristic feature of topological materials is the strong coupling of the spin and orbital momentum of Dirac electrons, which leads, in particular, to the fact that the directions of the spins of such electrons turn out to be rigidly tied to their direction of motion. This primarily applies to the parent electrons of the topological material. However, since the modification of the electronic properties of semiconductors or semimetals is carried out by introducing donor electrons or specific scattering centers into the material, the study of the behavior of donor electrons becomes almost of greater importance. The complexity of such a problem is exacerbated by the presence of orbital moments of the donor impurity. Therefore, initially [1,2] we undertook a study of the behavior of donor magnetic impurities with a purely spin state in a three-dimensional (3D) topological Dirac semimetal Cd_3As_2. It was noticed that there is a significant relationship between the spins of conduction electrons and localized purely spin states, leading, in particular, to an increase in the g-factor of the localized state and the appearance of a non-oscillating contribution to their interaction of Rudermann−Kittel−Kasui−Yosida (RKKY) [3–6]. From this naturally arises the question of the mutual influence of Dirac electrons and localized electronic states, which, along with the spin angular momentum, also have an orbital one. Theoretical calculations point to the opportunity of anisotropy in the RKKY interaction [7]. In the sphere of such interest, the study of the effect of chromium impurity on the properties of the 3D topological Dirac semimetal Cd_3As_2 was undertaken. The d-transition metal ions (Fe and Mn) with the $3d^5$ configuration are in the S-state, and their total orbital angular momentum is zero. Therefore, the magnetic state of these ions is traditionally considered to be purely spin with a g-factor equal to that of a free electron (2.0023). In case of a chromium impurity, which can be represented by a Cr^{2+} ion with a $3d^4$ configuration, and a Cr^{3+} ion with a $3d^3$ configuration, the magnetic states of the ions are not purely spin, and there is a significant contribution of the orbital angular momentum [8]. In addition, since the isovalent substitution of a Cd^{2+} ion by a Cr^{2+} ion does not directly produce donor Dirac electrons [9], the latter is associated with the formation of Cr^{3+}, mixed valence effects [10] and charge compensation violation. Thus, manifestations of the effects of the influence of the freedom orbital degree and various valence states hybridization of chromium ions with the wave functions of free electrons of the Cd_3As_2 matrix on its magnetic properties.

2. Experiment

Cd_3As_2 ingots doped with 0.45 at% Cr were synthesized at 1023 K as a direct interaction of the components: Cd (purity 99.999%), As (99.9999%) and Cr (99.99%), and through Cd−Cr alloys in glassy graphite crucibles placed in vacuum sealed quartz ampoules. The crystal structure and stoichiometry were confirmed by energy-dispersive analysis (EDX) and powder X-ray diffraction (PXRD), and repeat

the results reported in our works [1,2]. Electron paramagnetic resonance (EPR) was measured on a standard modulating Bruker EPR spectrometer in the X-band (9.3 GHz). The samples were paraffin-suspended powders of particles approximately 4 μm across. The cylindrical ampoule was rotated around its axis. Before measurements, the ampoule was held in a magnetic field 1.3 T at a temperature $\sim$ 370 K (above the melting point of paraffin) for 15 min and cooled to room temperature (until solidification of paraffin) in the same field.

3. Results and discussion

3.1. Crystal structure

As mentioned above, the PXRD data confirm the identity of the synthesized pure and doped compounds of the low-temperature tetragonal modification α-Cd_3As_2 [11] with symmetry space group $I4_1cd$ and parameters lattices $a = b = 12.653$ Å, $c = 25.456$ Å. The lattice parameters of pure α-Cd_3As_2 obtained in the same way were $a = b = 12.6539$ Å, $c = 25.4586$ Å. The experimental and calculated data as per PXRD, as well as in [1,2], practically coincide. It should be noted that each cm^3 α-Cd_3As_2 contains $2.564 \cdot 10^{20}$ crystal cells. The concentration of conduction electrons is only $6 \cdot 10^{17}$ cm^{-3}. And this is despite the fact that each cell contains 160 atoms, in particular, 96 Cd^{2+} ions and 64 As^{3-} ions in stoichiometric positions. In addition, the tetrahedral vacancies of the crystal cell, the main compositional motif of which is an antifluorite [12] type structure, can contain up to 0.16 at.% Cd^{2+} ions or, in the presence of impurities, ions Cr^{2+}. I.e. about 1 „extra“ atom of cadmium per six cells. However, the electrons from these cadmium ions do not enter the conduction band, since the possible concentration of such ions is 2 orders of magnitude higher than the electron concentration in a pure sample. The detachment energies of the second electrons Cd and Cr are very close. But for detachment of the third electron, significantly different energies are required: in the case of Cr^{2+} — 30.1 eV versus 37.5 eV for Cd^{2+} [13]. Divalent ion sizes $D_{Cd} \approx 1.98$ Å and $D_{Cr} \approx 1.66$ Å [13] also differ significantly and cause „subsidence“ of the lattice at the location of impurity chromium ions and, accordingly, contraction of bonds in the near coordination spheres.

3.2. Electron paramagnetic resonance

Based on general considerations on the opportunity of observing EPR on chromium ions [14], we can talk about the observation in our system of EPR on chromium ions Cr^{2+}, Cr^{3+}, Cr^{4+}. The chromium ion Cr^{2+} has the configuration $3d^4$ with spin $S = 2$ and orbital momentum $L = 2$, and its valence state completely corresponds to the substituted ion Cd^{2+}, as, for example, in the case of EPR in fluorite CaF_2 [15] and $CdGa_2S_4$ [16]. The chromium ion Cr^{4+} has the configuration $3d^2$ with $S = 1$. However, the formation of a Cr^{4+} ion due to the high detachment energy of the 4th electron in this system is incredible, as is its detection in the EPR measurements of the X-frequency range. Also, in this frequency range, it is impossible to observe EPR on the Cr^{2+} ion, which is obviously the main impurity when Cd_3As_2 is doped with chromium. Observation is impossible due to the strong splitting of the energy levels of this ion in the crystal field [14], which is larger than the RF field quantum. Thus, in the case of EPR measurements at frequencies in the X-range, only EPR on Cr^{3+} ions can be considered.

The EPR spectra of Cr^{3+} ions should have components corresponding to $S = 3/2$ and $L = 3$, which, in the case of low symmetry of the ion environment, decay into three components of the fine structure, a c in the case of the influence of the spin of the nucleus — also on the components of the hyperfine structure. The observed EPR spectrum is dominated by the resonance line, which has a distorted, almost symmetrical shape, in which traces of a fine or hyperfine structure can be seen (see Fig. 1). Note that although a natural mixture of chromium isotopes contains only 9% of an isotope with a non-zero nuclear spin (and this greatly reduces the intensity and the possibility of resolving the hyperfine structure), the manifestation of a super-hyperfine structure is also possible [17] caused by the interconfigurational interaction [18] with the nuclei of the Cd and As ligands, which in a natural mixture of isotopes contain nuclei with magnetic moments. Thus, the spectrum of the sample has a very complex structure, which allows us to state with a sufficient degree of confidence that the observed spectrum of the powder sample consists of minimum two groups of allowed EPR lines with a width of 300 Oe. Based on the results of experiments on doping α-Cd_3As_2 with other impurities, we associate these groups with Cr^{3+} ions located in the tetrahedral environment in the substitutional positions of the ions Cd^{2+} and in the positions of tetrahedral vacancies in the antifluorite structure [12]. However, most of these positions, in accordance with the level of doping, are occupied by Cr^{2+} ions, which, of course, affect the widths and positions of the EPR lines originating from Cr^{3+} ions.

In the temperature range of about 80−120 K, a plateau was observed in the EPR spectrum, which is characteristic of powder samples with an anisotropic g-factor. After a transient in the resonance field H_0 at $T \approx 120$ K, a rapid decrease H_0 was observed with decreasing temperature. This shift below 50 K was accompanied by a sharp broadening of the main resonance line. The temperature behavior of the EPR spectrum in our experiment requires a more painstaking presentation. The present paper, however, aims to report on a very important and interesting moment in this study — the observation of the angular dependence of the position and width of the EPR signal (see Fig. 1 and 2). Deal is that the sample is a powder with a particle size of approximately 4 μm, placed in paraffin and a cylindrical ampoule. The sample was rotated in a magnetic field around the ampoule axis. The Cr^{3+} ion is characterized by a slight anisotropy of the g-factor (typical values are

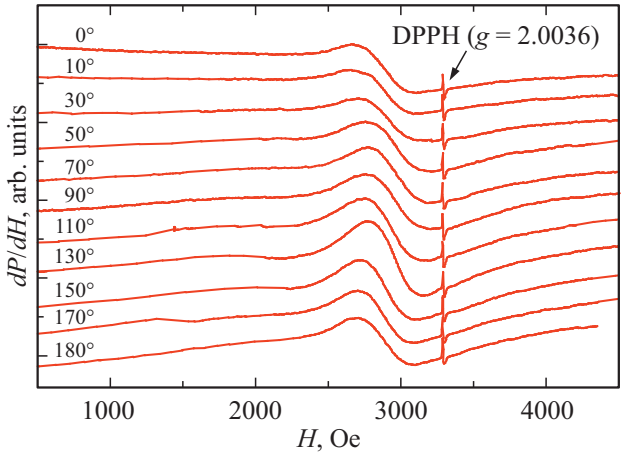

Figure 1. Variations in the EPR spectra during the rotation of the ampoule with powder around its axis. The vertical line refers to the standard marker diphenyl–picryl–hydrazyl (DPPH).

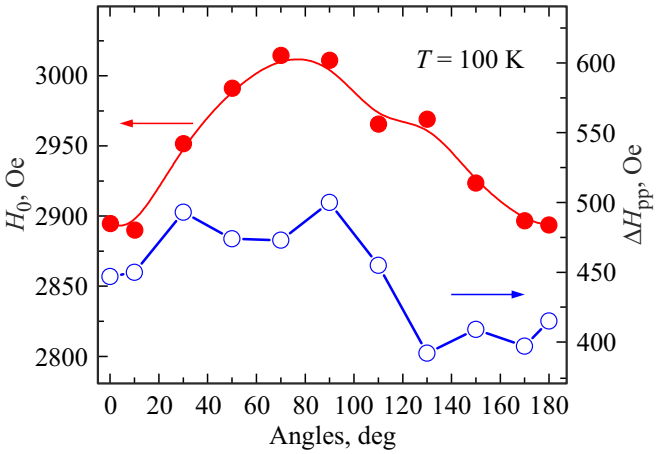

Figure 2. Dependences of the position H_0 and the peak-to-peak linewidth of EPR ΔH_{pp} on the angle of rotation of the ampoule around its axis.

$g_x, g_y, g_z \approx 1.95-1.98$). In our case (see Fig. 1) the g-factor ranges from 2.13 to 2.18. In case of a powder, where all crystallographic directions are equally probable, the ampoule rotation cannot lead to a change in the position of the EPR signal. In our experiment, the 2 angular dependences shown in Fig. 1 were obtained after paraffin melting and holding the sample for 15 min at a temperature of about ~ 380 K in a 13 kOe field and cooling in the same field until the paraffin solidifies. Angular dependencies indicate the presence of the 2nd axis, as well as in the work [19]. The same type of angular dependence is repeated in the line width. However, this does not directly indicate the nature of the anisotropy symmetry, since the particles are oriented only along the „direction of the easy axis“ (most likely, the c axis) when the orientation of other crystallographic axes is random. The fact that there is „an easy axis of magnetization“ in the paramagnetic state means that at a given temperature (~ 400 K) the value of the induced magnetization of chromium ions depends on the crystallographic direction. Let us emphasize that pure α-Cd_3As_2 is a strong diamagnet. The appearance of texture in a powder sample can be associated with only two factors: the magnetic anisotropy of the shape of the powder particles and the magnetic crystalline anisotropy. In the first case, the shape of the particles should again be tied to the crystal structure. For example, when preparing a powder, due to the pronounced cleavage of the crystal in the direction perpendicular to the c axis, disk-shaped particles (flakes) are formed. These particles in a magnetic field will line up with planes parallel to the field, even in the case of diamagnetism. The c axis will turn out to be perpendicular to the external magnetic field, and there will be disorder in the arrangement of the a and b axes. When preparing the powder, no pronounced manifestation of the cleavage plane was observed; although the powder particles were not spherical, they were characterized by similar sizes in three directions. Therefore, only the second factor remains significant — the presence of magnetic crystalline anisotropy in the paramagnetic state.

Thus, the orbital degrees of freedom significantly affect the magnetic state of the Cr^{2+} and Cr^{3+} ions, and in the case of Dirac quasiparticles, this effect can be expected to be enhanced due to the exchange interaction between localized magnetic moments and free Dirac electrons, the spins of which are rigidly related to their orbital moments. This results in an increase in the g-factor of localized magnetic moments and the appearance of an anisotropy of the induced magnetization in the paramagnetic state. Anisotropy manifests itself in the orientation of powder particles in a magnetic field even at temperatures ~ 400 K, which are noticeably higher than room temperature. At these temperatures, the positive magnetoresistance is still significant — both in pure and chromium-doped cadmium arsenide. In connection with this, it can be expected that, as in the case of doping with Mn^{2+} ions, magnetic polarons are formed on Cr^{2+} ions, which, however, will have anisotropic polarizability. Meanwhile, the source of donor electrons are the same Cr^{2+} ions, which donate one electron to the conduction band and turn into Cr^{3+} ions. Ions Cr^{3+}, on which EPR is observed, may have a stabilized valence, or may participate in a double exchange [10], the carriers of which in this case are donor Dirac electrons, the state of motion which are topologically protected. In this case, the lifetime of the Cr^{3+} and Cr^{2+} ions, or the exchange frequency, will affect the EPR linewidth and the phase of the Dirac electron wave function, which determines the modes of weak localization or antilocalizations [20–23]. This circumstance indicates the opportunity that the conditions for the implementation of the weak antilocalization regime will depend on the direction of motion of the Dirac electrons and, depending on the direction of the current, a positive [24] or a negative [25] magnetoresistance. Reducing the lifetime of the Cr^{3+} ion and its interaction with the conduction electron leads to a partial reduction in the

magnetic moment of the ion. And in case of a large g-factor of an electron, this causes a significant change in the g-factor of the ion.

Assuming that the value of the g-factor of the ion is the result of interaction with the magnetic moments of the current carriers, which reduce the magnetic moment, and using the results [26] for two interacting electronic subsystems with the corresponding g-factors g_1, g_2 and spins S_1, S_2,

$$g_{\text{eff}} = (g_1 S_1 + g_2 S_2)/(S_1 + S_2),$$

$$g_{\text{eff}} = g_{\text{Cr}}[1 - \mu(g_e/g_{\text{Cr}})]/(1 - \mu^*),$$

where $\mu^* = (\mu_{\text{Cr}} - \mu_0)/\mu_{\text{Cr}}$. For $g_e = 16$, $g_{\text{Cr}} = 2.0$, depending on the degree of reduction μ_{Cr}/μ_0 of the magnetic moment of the ion Cr^{3+}, we get the following effective g-factors: for $\mu_{\text{Cr}}/\mu_0 = 1.00$, $g_{\text{eff}} = 2.00$; for $\mu_{\text{Cr}}/\mu_0 = 0.99$, $g_{\text{eff}} = 2.154$.

It should also be taken into account that the Cr^{3+} ion is a jan-Teller ion [27–30], and local symmetry breaking of the tetrahedral envirroment of the ion in this topological material can be associated with it. This can also pin the magnetic moments of impurities in the crystal lattice and enhance the anisotropy in the paramagnetic state.

In addition, a few remarks about the opportunity of the presence in the sample of foreign phases or compounds from the Cr–As system, which, in principle, could give EPR signals and not be detected by other measurement methods. According to [31], in the Cr–As system there are 7 compounds with a melting temperature above or close to the synthesis temperature of Cd_3As_2 samples, which could remove chromium from investigated compound Cd_3As_2 and substitute its magnetic properties. Pure chromium is antiferromagnetic with a Neel temperature slightly above room temperature. However, for the compound with the highest chromium content, Cr_3As, an anomaly is observed in the temperature behavior of the magnetic susceptibility at 973 K. As the chromium content decreases, compounds with a complex magnetic structure are observed; however, naturally, the temperatures of magnetic transitions decrease. The Neel temperature for the sufficiently studied compounds Cr_2As and CrAs [32–38] is approximately 430 and 280 K, respectively. Thus, the magnetic transition temperature for the compound with the highest arsenic content $CrAs_2$ can be expected to be close to 200 K. In this range, there are no sharp features in the behavior of the EPR spectrum, which usually accompany phase transitions. This once again confirms the data on the composition and crystal structure of the samples: chromium dissolves well in α-Cd_3As_2 and does not form separate phases with each of the components during synthesis .

4. Conclusion

Thus, we believe that in EPR on Cr^{3+} ions in α-Cd_3As_2 there is an increase in the anisotropy of the paramagnetic susceptibility of localized spins ensemble of impurity chromium ions due to the orbital angular momentum and anisotropy of the g-factor of impurity ions interacting with the spin and anomalously large orbital momenta of donor Dirac electrons produced by the same impurity ions.

Funding

The study has been performed under the state assignments.

Conflict of interest

The authors declare that they have no conflict of interest.

References

[1] Yu.V. Goryunov, A.N. Nateprov. Phys. Solid State **62**, *1*, 100 (2020).
[2] Yu.V. Goryunov, A.N. Nateprov. Phys. Solid State **63**, *2*, 223 (2021).
[3] M.A. Ruderman, C. Kittel. Phys. Rev. **96**, *1*, 99 (1954).
[4] N. Bloembergen, T.J. Rowland. Phys. Rev. **97**, *6*, 1679 (1955).
[5] H.-R. Chang, J. Zhou, S.-X. Wang, W.-Y. Shan, D. Xiao. Phys. Rev. B **92**, *24*, 241103(R) (2015).
[6] J.-H. Sun, D.-H. Xu, F.-C. Zhang, Y. Zhou. Phys. Rev. B **92**, *19*, 195124 (2015).
[7] D. Mastrogiuseppe, N. Sandler, S.E. Ulloa. Phys. Rev. B **93**, *9*, 094433 (2016).
[8] S.A. Altshuler, B.M. Kozyrev. Elektronnyi paramagnitnyi rezonans soedineniy elementov promezhutochnykh grupp. Nauka, M. (1972). 672 p. (in Russian).
[9] B.A. Volkov, O.A. Pankratov. JETP Lett. **42**, *4*, 145 (1985).
[10] V.V. Bannikov, V.Ya. Mitrofanov. Phys. Solid State **47**, *8*, 1532 (2005).
[11] S. Borisenko, Q. Gibson, D. Evtushinsky, V. Zabolotnyy, B. Büchner, R.J. Cava. Phys. Rev. Lett. **113**, *2*, 027603 (2014).
[12] M.N. Ali, Q. Gibson, S. Jeon, B.B. Zhou, A. Yazdani, R.J. Cava. Inorg. Chem. **53**, *8*, 4062 (2014).
[13] A.I. Efimov, L.P. Belorukova, I.V. Vasilkova, V.P. Chechev. Svoystva neorganicheskikh soyedineniy. Khimiya, L. (1983), 392 p. (in Russian).
[14] D.A. Akhmetzyanov, V.B. Dudnikova, E.V. Zharikov, E.R. Zhiteitsev, O.N. Zaitseva, A.A. Konovalov, V.F. Tarasov. Phys. Solid State **55**, *3*, 520 (2013).
[15] P.B. Oliete, V.M. Orera, P.J. Alonso. Phys. Rev. **53**, *6*, 3047 (1996).
[16] A.G. Avanesov, V.V. Badikov, G.S. Shakurov. Phys. Solid State **45**, *8*, 1451 (2003).
[17] L.K. Aminov, I.N. Kurkin, B.Z. Malkin. Phys. Solid State **55**, *7*, 1343 (2013).
[18] A. Abragam. Phys. Rev. **79**, *3*, 534 (1950).
[19] I. Stefaniuk, M. Bester, I.S. Virt, M. Kuzma. Acta Phys. Polonica A **108**, *2*, 413 (2005).
[20] B.L. Al'tshuler, A.G. Aronov, A.I. Larkin, D.E. Khmel'nitskii. JETP **54**, *2*, 411 (1981).
[21] N.A. Abdullaev, O.Z. Alekperov, Kh.V. Aligulieva, V.N. Zverev, A.M. Kerimova, N.T. Mamedov. Phys. Solid State **58**, *9*, 1870 (2016).
[22] E.B. Olshanetsky, Z.D. Kvon, G.M. Gusev, N.N. Mikhailov, S.A. Dvoretsky, J.C. Portal. JETP Lett. **91**, *7*, 347 (2010).

[23] Y. Kumar, V.P.S. Awana. J. Supercond. Novel Magn. **34**, *5*, 1303 (2021). https://doi.org/10.1007/s10948-021-05910-1
[24] X. Yuan, P. Cheng, L. Zhang, C. Zhang, Y. Wang, Y. Liu, Q. Sun, P. Zhou, D.W. Chang, Z. Hu, X. Wan, H. Yan, Z. Li, F. Xiu. Nano Lett. **17**, *4*, 2211 (2017).
[25] Y. Liu, R. Tiwari, Z. Jin, X. Yuan, C. Zhang, F. Chen, L. Li, Z. Xia, S. Sanvito, P. Zhou, F. Xiu. Phys. Rev. B **97**, *8*, 085303 (2018).
[26] R.K. Wangsness. Phys. Rev. **91**, *5*, 1085 (1953).
[27] R. Rai, J.-Y. Savard, B. Tousignant. Canadian J. Phys. **47**, *11*, 69 (1969).
[28] J.J. Krebs, G.H. Stauss. Phys. Rev. B **15**, *1*, 17 (1977).
[29] M.G. Brik, N.M. Avram. J. Mol. Struct. **838**, *1–3*, 193 (2007).
[30] L. Seijo, Z. Barandiarán. J. Chem. Phys. **94**, *12*, 8158 (1991).
[31] M. Venkatraman, J.P. Neumann. Bull. Alloy Phase Diagrams **11**, *5*, 424 (1990).
[32] V.I. Valkov, A.V. Golovchan, U. Aparajita, O. Roslyak. Adv. Mater. Sci. Eng. 2019, Art. ID 9649628, Hindawi (2019). DOI: https://www.hindawi.com/journals/amse/2019/9649628/
[33] A.I. Popoola, Y.A. Odusote. J. Sustainable Technol. **10**, *2*, 63 (2019). ISSN: 2251-0680.
[34] B. Wang, Q. Lu, Y. Ge, K. Zhang, W. Xie, W.-M. Liu, Y. Liu. Phys. Rev. B **96**, *13*, 134116 (2017).
[35] H. Ofuchi, M. Mizuguchi, K. Ono, M. Oshima, H. Akinaga, T. Manago. Nucl. Instrum. Meth. Phys. Res. B **199**, 227 (2003).
[36] C. Autieri, C. Noce. Phil. Mag. **97**, *34*, 3276 (2017). https://doi.org/10.1080/14786435.2017.1375607
[37] R. Khasanov, Z. Guguchia, I. Eremin, H. Luetkens, A. Amato, P.K. Biswas, C. Rüegg, M.A. Susner, A.S. Sefat, N.D. Zhigadlo, E. Morenzoni. Sci. Rep. **5**, 13788 (2015). DOI: 10.1038/srep13788
[38] G. Cuono, C. Autieri, G. Guarnaccia, A. Avella, M. Cuoco, F. Forte, C. Noce. Eur. Phys. J. Spec. Top. **228**, 631 (2019).

Translated by E.Potapova